Nuclear Medicine and Biology 40 (2013) 823–830

Contents lists available at SciVerse ScienceDirect

Nuclear Medicine and Biology

journal homepage: www.elsevier.com/locate/nucmedbio

In vivo comparison of DOTA based ^{68}Ga-labelled bisphosphonates for bone imaging in non-tumour models

Marian Meckel [a], Marco Fellner [a], Natalie Thieme [b], Ralf Bergmann [b], Vojteck Kubicek [c], Frank Rösch [a,*]

[a] Institute of Nuclear Chemistry, Johannes-Gutenberg-University Mainz, Fritz-Strassmann-Weg 2, 55128 Mainz, Germany
[b] Institute of Radiopharmacy, Helmholtz-Zentrum Dresden-Rossendorf, Bautzner Landstraße 400, 01328 Dresden, Germany
[c] Department of Inorganic Chemistry, Charles University Prague, Hlavova 2030, 12840 Prague, Czech Republic

ARTICLE INFO

Article history:
Received 1 February 2013
Received In revised form 26 April 2013
Accepted 29 April 2013

Keywords:
Bone metastases
^{68}Ga
PET
^{177}Lu
DOTA
Bisphosphonates

ABSTRACT

Bone metastases are a class of cancerous metastases that result from the invasion of a tumor into bone. The solid mass which forms inside the bone is often associated with a constant dull ache and severe spikes in pain, which greatly reduce the quality of life of the patient. Numerous ^{99m}Tc-labeled bisphosphonate functionalised complexes are well established tracers for bone metastases imaging. The objective of this research was to evaluate the pharmacokinetics and behaviour of three DOTA based bisphosphonate functionalised ligands (BPAMD, BPAPD and BPPED), using both ^{68}Ga μ-PET *in vivo* imaging and *ex vivo* biodistribution studies in healthy Wistar rats. The compounds were labelled with ^{68}Ga in high yields using an ammonium acetate buffer, and subsequently purified using a cation exchange resin. High bone uptake values were observed for all ^{68}Ga-labelled bisphosphonates at 60 minutes p.i. The highest uptake was observed for [^{68}Ga]BPPED (2.6 ± 0.3% ID/g) which compares favourably with that of [^{99m}Tc]MDP (2.7 ± 0.1 ID/g) and [^{18}F]fluoride (2.4 ± 0.2% ID/g). The ^{68}Ga-labelled DOTA-bisphosphonates showed rapid clearance from the blood and renal system, as well as low binding to soft tissue, resulting in a high bone to blood ratio (9.9 at 60 minutes p.i. for [^{68}Ga]BPPED, for example). Although further studies are required to assess their performance in tumor models, the results obtained suggest that these ligands could be useful both in imaging (^{68}Ga) and therapeutic treatment (^{177}Lu) of bone metastases.

1. Introduction

Together with the lungs and liver, the bones are most frequently affected by metastases. A significant portion (60–80%) of bone metastases are caused by breast or prostate carcinoma. The formation usually occurs at the early stages of tumour development; however, their symptoms are only recognized at later stages [1,2]. For this reason the none-invasive diagnosis of bone metastases in a premature state, which allows for a profound and timely decision on subsequent therapy, is of great importance to improving the quality of life of the patients. ^{99m}Tc-labelled bisphosphonate functionalised ligands are well established for SPECT/CT imaging of osteoblastic metastases [3]. The resolution and sensitivity of metastases imaging would be significantly enhanced if a positron emitter was to be used instead, of which there are only a few examples. The inherent advantages of PET/CT, over the SPECT/CT, is clearly demonstrated by using [^{18}F]fluoride ([^{18}F]F$^-$) [4]. The images obtained with [^{18}F]F$^-$ are far superior to those obtained using ^{99m}Tc-radiopharmaceuticals. There is considerable interest in ^{68}Ga-labelled complexes as an alternatives to [^{18}F]F$^-$.

Bisphosphonates are known to show high and fast binding to apatite (bone) structures [5]. Commonly used ^{99m}Tc-labelled phosphonates include methylene diphosphonate (MDP), dicarboxypropane diphosphonate (DPD) and hydroxymethylene diphosphonate (HDP). Chemically attaching these bisphosphonates to a positron emitter is of great interest and potential for the *in vivo* imaging of bone metastases using PET/C. Combining the bisphosphonate targeting moieties with the macrocyclic ligand DOTA, an established ligand for use in ^{68}Ga-PET, led to a new generation of radiolabeled bisphosphonates. In addition to the benefits associated with the application of the PET radionuclide, in particular ^{68}Ga, the DOTA-bisphosphonates also have the potential to be used in therapeutic applications. DOTA is known to form complexes, which are stable *in vivo*, with a range of metal cations, and therefore DOTA-bisphosphonates could also be labelled with therapeutic nuclides (such as ^{177}Lu for example). In this way a single DOTA-bisphosphonate structure may have the potential to be used for both imaging and therapy of bone metastases simply by changing the radionuclide incorporated. This is a significant advantage over the [^{18}F]F$^-$, [^{153}Sm]EDMTP and [^{99m}Tc]MDP/[^{153}Sm]EDMTP systems. In

* Corresponding author. Tel.: +49 6131 392 5302; fax: +49 6131 392 5879.
E-mail address: Frank.Roesch@uni-mainz.de (F. Rösch).

0969-8051/$ – see front matter © 2013 Elsevier Inc. All rights reserved.
http://dx.doi.org/10.1016/j.nucmedbio.2013.04.012

general terms, this 2-in-1 "theranostic" approach has a number of significant advantages (commercially and in practice) and is of considerable commercial interest.

One of the more promising DOTA conjugated bisphosphonates, (4-{[bis-(phosphonomethyl) carbamoyl] methyl}-7,10-bis(carboxymethyl)-1,4,7,10-tetraazacyclo-dodec-1-yl) acetic acid (BPAMD), has already been labelled using ^{68}Ga, to give the PET tracer [^{68}Ga]BPAMD [6]. Very promising initial human studies have been reported for this tracer following evaluation in a patient with extensive bone metastases arising from prostate cancer [7]. In this evaluation [^{68}Ga]BPAMD provided excellent imaging of bone metastases with very high bone to soft tissue ratios and fast clearance (no detectable blood pool and very faint renal activity). PET/CT depicted multiple, intense osteoblastic metastases in the entire skeleton, with a maximum standardised uptake value (SUV_{max}) of 77.1 in the 10th thoracic vertebra and an SUV of 62.1 for vertebra L2. These values are superior to those quantified for the same vertebra, 39.1 and 39.2 respectively, when the PET/CT was performed in the same patient using [^{18}F]F^-.

Following the very favourable and promising results obtained with [^{68}Ga]BPAMD, two further DOTA-bisphosphonate derivatives have been described recently in the search for even better structures [8]. How these derivatives compare to [^{68}Ga]BPAMD has not yet been addressed, and is the subject of the present study. *In vivo* PET/CT studies and systematic biodistribution experiments have been carried out for each of these three ^{68}Ga-labelled DOTA-bisphosphonates. The results obtained for these ^{68}Ga-labelled compounds have been compared with [^{18}F]F^- and [^{99m}Tc]MDP.

2. Materials and methods

2.1. Generator

Decay of Germanium-68 ($t_{1/2}$ = 270.8 d) provides an easily available source of the PET nuclide Gallium-68 ($t_{1/2}$ = 67.71 min). Germanium-68 is fixed on a solid phase of modified titanium dioxide, and Gallium-68 eluted from the generator with 10 mL 0.1 M HCl. This is followed by immobilisation of the ^{68}Ga on an acidic cation exchanger. Impurities such as zinc, iron and titanium as well as ^{68}Ge generator breakthrough are removed using a mixture of acetone and hydrochloric acid. Subsequently, ^{68}Ga is quantitatively eluted with 1 M HCl (300 μL) from the cation exchanger. This eluate serves as an ideal low-volume and chemically highly pure source of ^{68}Ga for subsequent labelling [9,10].

2.2. DOTA-bisphosphonates

The following macrocyclic DOTA based bisphosphonate chelators have been used (see Fig. 1 for their chemical structures): BPAMD (4-{[(bis-phosphonomethyl) carbomoyl]methyl}-7,10-bis-(carboxymethyl)-1,4,7,10-tetraazacyclododec-1-yl)-acetic acid, BPAPD (4-{[(bis–phosphonopropyl)carbomoyl]methyl}-7,10-bis-(carboxymethyl)-1,4,7,10-tetraazacyclododec-1-yl)-acetic acid and BPPED tetraethyl-10-{[(2,2-bis-phosphonoethyl)hydroxyphosphoryl]methyl}-1,4,7,10-tetraazacyclododecane-1,4,7-triacetic acid. According to a different terminology, these ligands are also denoted as $DOTAM^{BP}$, $DOTAP^{BP}$ and $DO3AP^{BP}$. The ligands were synthesized following literature procedures [6,8] (Fig. 2).

2.3. Labeling

^{68}Ga labeling was performed in an ammonium acetate solution (2 M, 200 μL) by adding 300 μL of processed ^{68}Ga, giving a labeling pH of 3.75. The ligand (30 nmol) was added and the solution shaken in a heating block for 10 min at 100 °C. After cooling, the labeled bisphosphonate was separated from un-complexed ^{68}Ga by passing the solution over a strong cation exchange resin (STRATA X-C, Phenomenex). The pH was adjusted to pH = 7 by adding small amounts of a 1 M NaOH solution. The radiochemical yield was determined by radio-TLC (solid phase: SiO_2, 60 F_{254}, Merck) using a mixture of 2 parts A (conc. HCl, acetone, water) and 1 part B (acetylacetone) as the mobile phase. The radioactivity distribution on the TLC plates was determined on a Canberra Packard Instant Imager. The reaction was also monitored via radio-HPLC (SCX-column, solvent: 1 M phosphate buffer, pH = 3). The labeled bisphosphonates were obtained in radiochemical purities greater than 95%, after resin purification [11].

No-carrier-added aqueous [^{18}F]F^- was obtained from an IBA CYCLONE 18/9 cyclotron (IBA, Louvain-la-Neuve, Belgium) by irradiation of [^{18}O]H_2O via the ^{18}O(p,n)^{18} F nuclear reaction. [^{18}F]F^- was dissolved in electrolyte injection solution E-153 (Serumwerk Bernburg AG).

[^{99m}Tc]$NaTcO_4$ was obtained from a commercial ^{99}Mo/^{99m}Tc-generator (Covidien) and [^{99m}Tc]MDP was produced according to the manufacturer procedure (ROTOP Pharmaka AG).

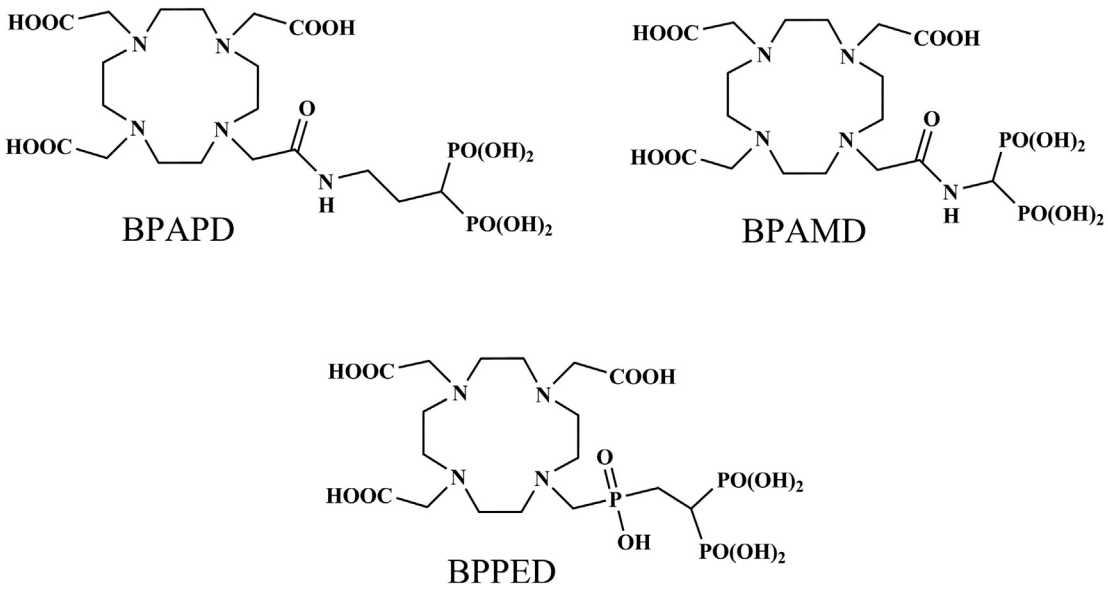

Fig. 1. Structures of the DOTA functionalised bisphosphonate derivatives.

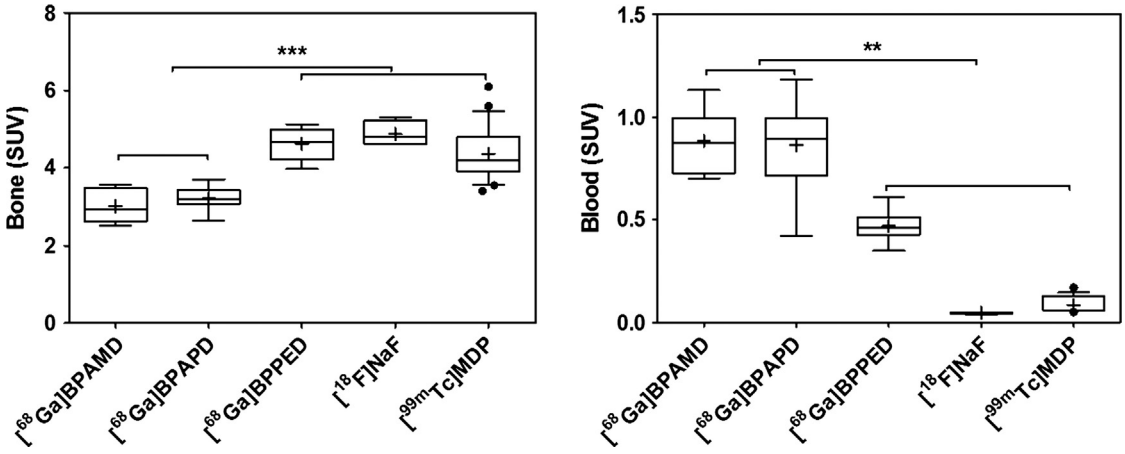

Fig. 2. Comparison of [^{68}Ga]BPAMD, [^{68}Ga]BPAPD, [^{68}Ga]BPPED [^{18}F]NaF and [^{99m}Tc]MDP. The graph on the left represents the SUV of the bone at 60 min p.i., and the right hand side graph represents the SUV of the blood at 60 min p.i.

2.4. Animals, feeding, husbandry, and animal preparation

The local animal research committee at the Landesdirektion Dresden approved the animal facilities and the experiments according to institutional guidelines and the German animal welfare regulations. The experimental procedure used conforms to the *European Convention for the Protection of Vertebrate Animals used for Experimental and other Scientific Purposes (ETS No. 123)*, to the *Deutsches Tierschutzgesetz*, and to the *Guide for the Care and Use of Laboratory Animals* published by the US National Institutes of Health [DHEW Publication No. (NIH) 82-23, revised 1996, Office of Science and Health Reports, DRR/NIH, Bethesda, MD 20205]. Wistar rats (Wistar Unilever, HsdCpb:WU, Harlan Winkelmann, Borchen, Germany) were housed under standard conditions with free access to food (2016 Teklad Global 16% Protein Rodent Diet, Harlan Laboratories, Inc., Germany) and tap water. Rats were housed (5 rats per cage) in Uni Protect airflow cabinet (Ehret GmbH Labor- und Pharmatechnik, Schönwalde, Germany) in polysulfone cages (380 × 200 × 590 mm; floor area, 1815 cm^2). The caging had a solid bottom and stainless steel wire lid, and the cage floor was covered with chipped wood. The cages were changed weekly. Tap water was provided in polycarbonate bottles, changed twice weekly, and refilled once between the cage changes. The room temperature was 22 ± 1 °C and relative humidity was 53 ± 6%, but the temperature was 1–4 °C higher in the airflow cabinets. Artificial lighting was in 12 h light and dark cycles with fluorescent tubes (light color, warm white).

2.5. Surgery

Male Wistar-Unilever rats weighing 183 ± 56 g (mean ± SD, n = 19) were anesthetized using desflurane. The guide value for breathing frequency was 65 breaths/min. Animals were put in the supine position and placed on a heating pad to maintain body temperature. The rats were treated with 100 units/kg heparin (Heparin-Sodium 25.000-ratiopharm, Ratiopharm, Germany) by subcutaneous injection to prevent blood clotting on intravascular catheters. After local anesthesia by injection of Lignocaine 1% (Xylocitin loc, Mibe, Jena, Germany) into the right groin, catheter was introduced into the right femoral artery (0.8 mm Umbilical Vessel Catheter, Tyco Healthcare, Tullamore, Ireland) for blood samples for metabolite analysis, for gas analysis, and arterial blood pressure measurements. A second needle (35 G) catheter in one tail vein was used for administration of the tracers.

2.6. Metabolite analysis

The metabolism of [^{68}Ga]BPAPD, [^{68}Ga]BPAMD, [^{68}Ga]BPPED *in vivo* was analyzed in arterial blood plasma samples. The radiotracer was injected intravenously into anesthetized male Wistar rats. Blood samples from the right femoral artery were taken using the catheter at various time points up to 120 min post injection (p.i.). Plasma was separated by centrifugation (3 min, 11 000 g) followed by precipitation of the plasma proteins with ice-cold methanol (1.5 parts per 1 part plasma) and centrifugation (3 min, 11 000 g). The supernatants were analyzed by TLC on cellulose (Merck KGaA, Darmstadt, Germany) with a mixture of 2 volume parts solution A) H_2O (9 mL), 12 M HCl (0.6 mL), acetone (88 mL), and one volume part B) acetylacetone. A second TLC system was used to determine free ^{68}Ga with silica TLC-plates (Nano-Sil-20, Macherey-Nagel, Germany) with citrate buffer (0.24 M, pH 4). The metabolite fraction of the arterial blood plasma activity was calculated using the fraction of parent compound by the equation metfrac = 1 − parent fraction. The chemical nature of the radioactive metabolites was not evaluated.

2.7. Biodistribution studies

Biodistribution studies were performed in male Wistar rats. The rats were injected intravenously, each with ~ 10 MBq of the ^{68}Ga-labeled compound in 0.5 mL saline. Specific details are as follows. [^{68}Ga]BPAPD: 63 ± 13 MBq/kg, 123 ± 16 body-weight (BW, g), n = 16; [^{68}Ga]BPAMD: 67 ± 7 MBq/kg, 146 ± 14 BW (g), n = 16; [^{68}Ga]BPPED: 82 ± 28 MBq/kg, 148 ± 12 BW (g), n = 16; [^{99m}Tc]MDP: 1 MBq/kg, 204 ± 5 (g), n = 6; [^{18}F]F$^-$: 7.0 ± 0.5 MBq/kg, 183 ± 12 BW (g), n = 8. Animals were sacrificed at 5 and 60 min p.i for [^{18}F]F$^-$ and the ^{68}Ga-labeled tracers, and 5 and 120 min for [^{99m}Tc]MDP. Organs and tissues of interest were excised rapidly, weighed, and the radioactivity determined using a Wallac WIZARD automatic gamma counter (PerkinElmer, Germany). The activity of the tissue samples was decay-corrected and calibrated by comparing the counts in the tissue with the counts in aliquots of the injected tracer. Counts of the sample and calibration aliquots were measured in the gamma counter at the same time. The amount of activity in the selected tissues and organs is expressed as a percent of the injected dose per organ (% ID) or activity concentration normalized to the BW as the SUV [(activity per g tissue)/(injected activity) × BW]. Values are quoted as the mean ID % ± standard deviation (SD) of the eight rats per group. The activity associated with the skeleton was calculated using the activity concentration in the femur and the total skeleton weight, calculated using: skeleton weight = 9.66 + 0.0355 × BW [12].

2.8. Small animal PET

In vivo small animal PET imaging in male Wistar rats was carried out under general anesthesia of the rats (induced with 10% and

Table 1
Activity (% ID, mean ± SD of n animals) at different ROI's of Wistar rats for [^{68}Ga]BPAMD, [^{68}Ga]BPAPD, [^{68}Ga]BPPED and [^{18}F]F$^-$.

	[^{68}Ga]BPAPD			[^{68}Ga]BPAMD			[^{68}Ga]BPPED			[^{18}F]Fluoride		
	5 min			5 min			5 min			5 min		
	mean	SD	n	mean	SD	n	mean	SD	n	mean	SD	n
Brain	0.10	0.04	8.00	0.07	0.01	8.00	0.05	0.01	8.00	0.05	0.05	4.00
Pancreas	0.10	0.03	8.00	0.08	0.01	8.00	0.09	0.02	8.00	0.06	0.01	4.00
Spleen	0.09	0.02	8.00	0.07	0.01	8.00	0.07	0.01	8.00	0.08	0.01	4.00
Adrenals	0.02	0.00	8.00	0.02	0.00	8.00	0.02	0.01	8.00	0.01	0.00	4.00
Kidneys	3.38	0.91	8.00	2.94	1.04	8.00	3.12	0.69	8.00	1.55	0.58	4.00
Heart	0.30	0.06	8.00	0.27	0.06	8.00	0.20	0.03	8.00	0.12	0.00	4.00
Lung	0.73	0.22	8.00	0.61	0.09	8.00	0.53	0.09	8.00	0.30	0.03	4.00
Thymus	0.16	0.04	8.00	0.12	0.02	8.00	0.15	0.04	8.00	0.17	0.02	4.00
Thyroide	0.07	0.01	8.00	0.06	0.01	8.00	0.07	0.02	8.00	0.07	0.01	4.00
Harderian glands	0.08	0.01	8.00	0.08	0.01	8.00	0.06	0.01	8.00	0.04	0.01	4.00
Liver	3.53	0.51	8.00	2.96	0.40	8.00	2.68	0.35	8.00	1.44	0.10	4.00
Femur	1.38	0.20	8.00	1.29	0.09	8.00	1.91	0.13	8.00	1.74	0.14	4.00
Testes	0.53	0.08	8.00	0.47	0.08	8.00	0.53	0.08	8.00	0.24	0.05	4.00
Intestine	2.29	0.25	8.00	1.97	0.18	8.00	2.08	0.22	8.00	1.48	0.18	4.00
Stomach	0.58	0.10	8.00	0.43	0.03	8.00	0.52	0.13	8.00	0.19	0.03	4.00
Skeleton	26.21	3.87	8.00	22.71	3.09	8.00	34.21	3.16	8.00	26.60	2.14	4.00
Urine calculated	14.91	0.94	4.00	8.98	5.90	4.00	10.40	7.53	8.00	7.87	6.78	4.00

Data recorded at 5 min p.i.

maintained with inhalation of 6.5% desflurane in 30% oxygen/air), with a scan time of 120 min. Rats were immobilized in the supine position, with their medial axis parallel to the axial axis of the scanner (microPET® P4, Siemens Medical Solutions, Knoxville, TN, USA). In the PET experiments 0.5 mL of the tracers ([^{68}Ga]BPAPD: n = 2, 341 ± 21 MBq/kg; [^{68}Ga]BPAMD: n = 3, 265 ± 30 MBq/kg; [^{68}Ga]BPPED: n = 2, 232 ± 75 MBq/kg; [^{18}F]F : n = 1, 77.8 MBq/kg) was administered via a tail vein as an infusion (0.5 mL/min) using a syringe pump (Harvard Apparatus, Holliston, MA, USA) and a needle catheter. Transmission scans and PET acquisition followed, details of which have been published elsewhere [13]. No correction for partial volume effects was applied. The image volume data were converted to Siemens ECAT7 format for further processing, and the image files processed using ROVER software (ABX GmbH, Radeberg, Germany). Masks for defining three-dimensional regions of interest were set and the regions of interest (ROI's) defined by thresholding. ROI time activity curves (TAC) were derived for the subsequent data analysis. The ROI data and TAC were further analyzed using R (R is available as Free Software under the terms of the Free Software Foundation's GNU General Public License in source code form) and specifically developed program packages. SUV's (mL/g) were calculated for the ROI's using the equation: SUV = (activity/mL tissue)/(injected activity/body weight).

2.9. Small animal SPECT

In vivo small animal SPECT imaging in a male Wistar rat was carried out under general anesthesia (induced with 10% and maintained with inhalation of 6.5% desflurane in 30% oxygen/air) with a scan time of 120 min. The rat was immobilized in the prone position with the medial axis parallel to the axial axis of the SPECT scanner (NanoSPECT, Bioscan Inc., Washington, D.C., USA).The camera was fitted with four nine-pin-hole apertures. The pinhole diameters were 2.5 mm and allow a resolution of ~ 1.6 mm in rat-sized animals. [^{99m}Tc]MDP (0.5 mL, 322 MBq/kg, n = 1) was administered via a tail vein as an infusion (0.5 mL/min) using a syringe pump (Harvard Apparatus, Holliston, Ma, USA) and a needle catheter. Data was acquired in a step-and-shoot mode with the bed also stepping to include the complete rat within the field of view. An energy window was used for ^{99m}Tc with a peak at 140 keV. The SPECT acquisitions were reconstructed using InVivoScope 1.37 software (Bioscan) with a voxel size of 0.8 mm, using the ordered subsets expectation maximization iterative reconstruction algorithm with four subsets and six iterations. During reconstruction, high noise suppression was selected to produce smoother and more artifact-free images. The DICOM datasets were converted to ECAT7 format and analyzed as per

Table 2
Activity (% ID, mean ± SD of n animals) at different ROI's of Wistar rats for [^{68}Ga]BPAMD, [^{68}Ga]BPAPD, [^{68}Ga]BPPED, [^{18}F]F$^-$ (60 min p.i.) and [^{99m}Tc]MDP (120 min p.i.).

	[^{68}Ga]BPAPD			[^{68}Ga]BPAMD			[^{68}Ga]BPPED			[^{18}F]Fluoride			[^{99m}Tc]MDP		
	60 min			60 min			60 min			60 min			120 min		
	mean	SD	n	mean	SD	n	mean	SD	n	mean	SD	n	mean	SD	n
Brain	0.05	0.02	8.00	0.04	0.01	8.00	0.03	0.02	8.00	0.01	0.00	4.00	0.01	0.02	6.00
Pancreas	0.05	0.02	8.00	0.10	0.14	8.00	0.08	0.09	8.00	0.03	0.03	4.00	0.01	0.00	6.00
Spleen	0.06	0.02	8.00	0.10	0.09	8.00	0.06	0.03	8.00	0.02	0.04	4.00	0.01	0.00	6.00
Adrenals	0.02	0.01	8.00	0.01	0.01	8.00	0.01	0.00	8.00	0.00	0.00	4.00	0.00	0.00	6.00
Kidneys	0.58	0.08	8.00	0.58	0.03	8.00	0.56	0.34	8.00	0.09	0.01	4.00	0.60	0.03	6.00
Heart	0.14	0.06	8.00	0.12	0.01	8.00	0.07	0.01	8.00	0.01	0.00	4.00	0.01	0.00	6.00
Lung	0.32	0.08	8.00	0.25	0.05	8.00	0.17	0.03	8.00	0.03	0.01	4.00	0.06	0.02	6.00
Thymus	0.11	0.03	8.00	0.08	0.02	8.00	0.05	0.01	8.00	0.02	0.01	4.00	0.01	0.00	6.00
Thyroide	0.04	0.01	8.00	0.03	0.01	8.00	0.03	0.01	8.00	0.04	0.02	4.00	0.02	0.01	6.00
Harderian glands	0.08	0.03	8.00	0.06	0.02	8.00	0.05	0.01	8.00	0.01	0.00	4.00	0.01	0.01	6.00
Liver	1.95	0.45	8.00	2.00	0.37	8.00	1.10	0.23	8.00	0.09	0.02	4.00	0.26	0.03	6.00
Femur	2.09	0.15	8.00	1.68	0.16	8.00	2.58	0.33	8.00	2.71	0.09	4.00	2.36	0.17	6.00
Testes	0.33	0.10	8.00	0.33	0.09	8.00	0.17	0.02	8.00	0.05	0.00	4.00	0.03	0.00	6.00
Intestine	1.93	0.37	6.00	1.76	0.62	8.00	2.56	1.78	8.00	1.13	0.18	4.00	6.57	2.87	6.00
Stomach	1.79	2.61	8.00	0.30	0.14	8.00	2.94	5.85	8.00	0.15	0.20	4.00	1.55	1.61	6.00
Skeleton	38.31	5.01	8.00	30.90	4.14	8.00	48.90	4.82	8.00	43.70	1.93	4.00	41.22	5.61	6.00
Urine calculated	25.93	7.34	8.00	42.20	5.11	8.00	31.90	9.84	8.00	24.30	2.83	4.00	38.10	4.11	6.00

the small animal PET protocol. The total counts within this volume were then converted to activity using a predetermined calibration factor. The CT acquisition was carried out in a SkyScan 1178 (SkyScan, Belgium) and was reconstructed at standard resolution.

2.10. Statistical analysis

Continuous variables were expressed as the mean ± SD. Normality was assessed using the D'Agostino-Pearson normality test. Groups were compared using the Student t test or the Mann-Whitney U test, as appropriate. All statistical tests were 2-tailed, with a P value of less than 0.05 denoting significance, the symbols represent $^{*}P < 0.05$, $^{**}P < 0.01$, $^{***}P < 0.001$. All statistical analyses were performed using GraphPad Prism (V5.02 for Windows, GraphPad Software, San Diego, CA, USA, www.graphpad.com).

3. Results

3.1. Radiolabeling

The DOTA conjugated bisphosphonates were labeled with ^{68}Ga, and isolated with high radiochemical purities of 95–98% after purification.

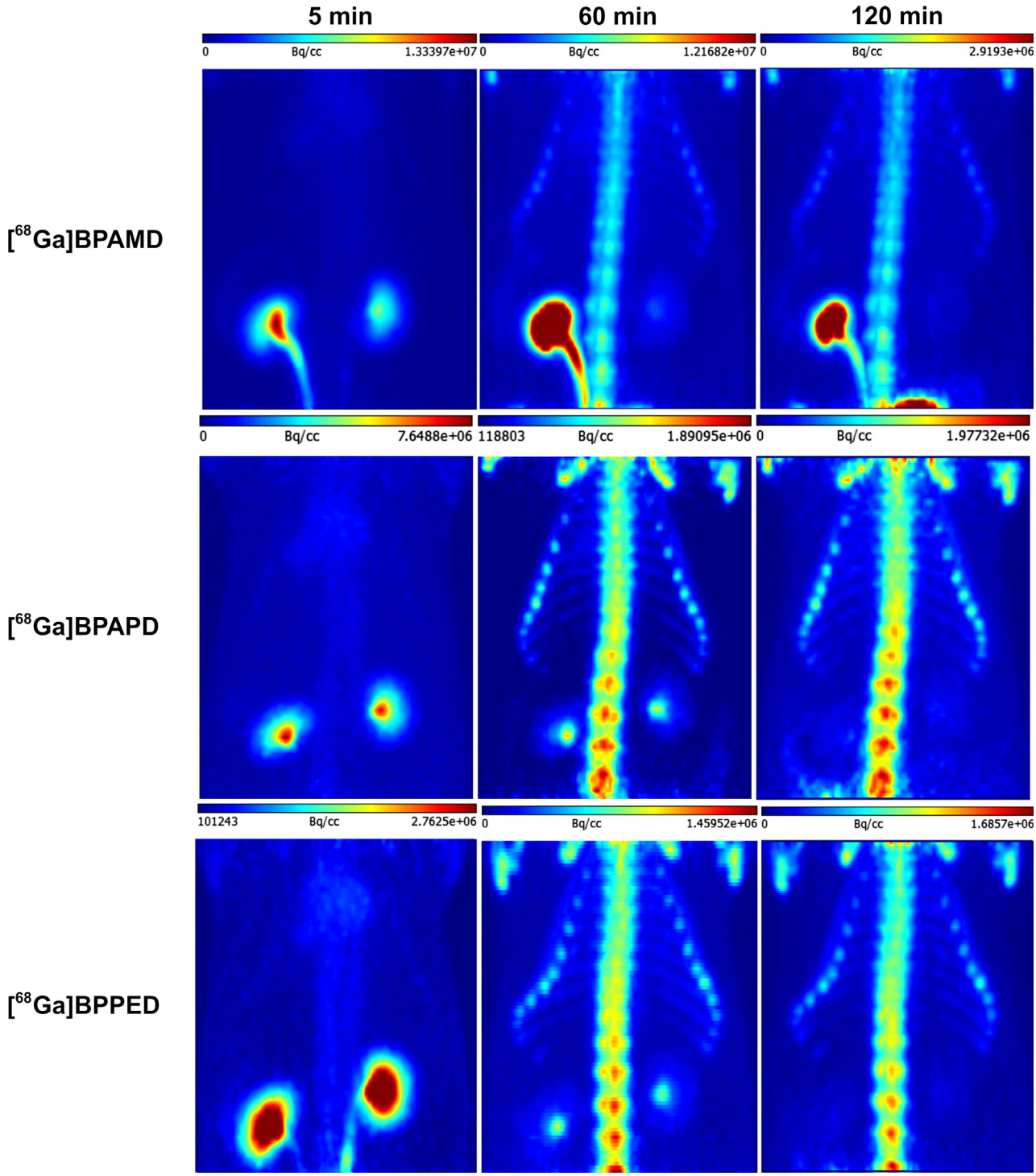

Fig. 3. MIP (maximum intensity projection) in the thorax region for [^{68}Ga]BPAMD, [^{68}Ga]BPAPD and [^{68}Ga]BPPED at 5 min, 60 min and 120 min p.i.

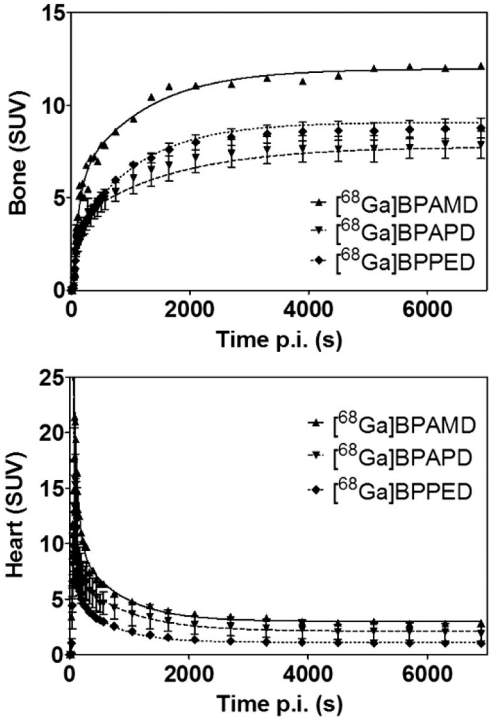

Fig. 4. Accumulation of the DOTA functionalised bisphosphonates in the spine (upper) of the rats and clearance from the blood (lower, ROI: over the heart).

3.2. Biodistribution

The biodistribution data of [^{68}Ga]-DOTA-bisphosphonates, [^{18}F]F$^-$ and [^{99m}Tc]MDP studied in normal Wistar rats are presented in tables 1 and 2. All radiotracers investigated showed a high degree of association with the bone. The detailed analysis of the activity associated with the bones reveals a significantly ($P < 0.001$) higher level of [^{68}Ga]BPPED, [^{18}F]F$^-$, and [^{99m}Tc]MDP accumulation compared to [^{68}Ga]BPAMD and [^{68}Ga]BPAPD. This is also evident from the estimation of the total activity in the skeleton for [^{68}Ga]BPAPD (38% ID), [^{68}Ga]BPAMD (31% ID), [^{68}Ga]BPPED (49% ID), [^{18}F]F$^-$ (44% ID), and [^{99m}Tc]MDP (41% ID) at the end of the scan. The tracers showed fast renal elimination and high clearance from the blood, which is presumably a result of their high hydrophilicity. PET Scans were conducted over 60 min p.i. for the [^{68}Ga]-DOTA-bisphosphonates and [^{18}F]F$^-$, and 120 min p.i. for [^{99m}Tc]MDP. The bone to blood ratios determined at the end of the scan were [^{68}Ga]BPAMD 3.4; [^{68}Ga]BPAPD 3.7; [^{68}Ga]BPPED 9.9; [^{18}F]F$^-$ 103; [^{99m}Tc]MDP 52.3. The measured urine activity was 26% ID for [^{68}Ga]BPAPD, 42% ID for [^{68}Ga]BPAMD, 49% ID for [^{68}Ga]BPPED, 44% ID for [^{18}F]fluoride, and 41% ID for [^{99m}Tc]MDP at the end of the respective scans. The summed activity in the skeleton and urine was 64% ID for [^{68}Ga]BPAPD, 73% ID for [^{68}Ga]BPAMD, 81% ID for [^{68}Ga]BPPED, 68% ID for [^{18}F]F$^-$, and MDP 79% ID for [^{99m}Tc]. In all cases the activity concentration in the other tissues and organs was very low, and there was no visible activity accumulation observed in the brain or liver (Tables 1 and 3).

3.3. Small animal PET

The *in vivo* PET data are summarized in Fig. 3. [^{68}Ga]BPAMD, [^{68}Ga]BPAPD and [^{68}Ga]BPPED were accumulated fast in the skeleton, reaching a plateau after one hour. The distribution half-lives of the radiotracers in the circulation were between one and two min, which correlates to the blood circulation time in rats. The half-lives of the slow components were 13 min for [^{68}Ga]BPAMD, 19 min for [^{68}Ga]BPAPD and 12 min for [^{68}Ga]BPPED. The measured target to background ratios were equal to the established standards in bone imaging set by [^{18}F]F and [^{99m}Tc]MDP (Fig. 4). Fig. 5 shows the distribution kinetics of [^{18}F]F$^-$, [^{68}Ga]BPAMD, [^{68}Ga]BPAPD, and [^{68}Ga]BPPED in the heart, kidney, spine and blood (vein) (Table 2). The curves are similar for all compounds. Variations in the curve profiles of the kidney time activity curves seems to be a result of the differing responses of individual rats to anesthesia, and resulting differences in the urine flow between rats (Fig. 6).

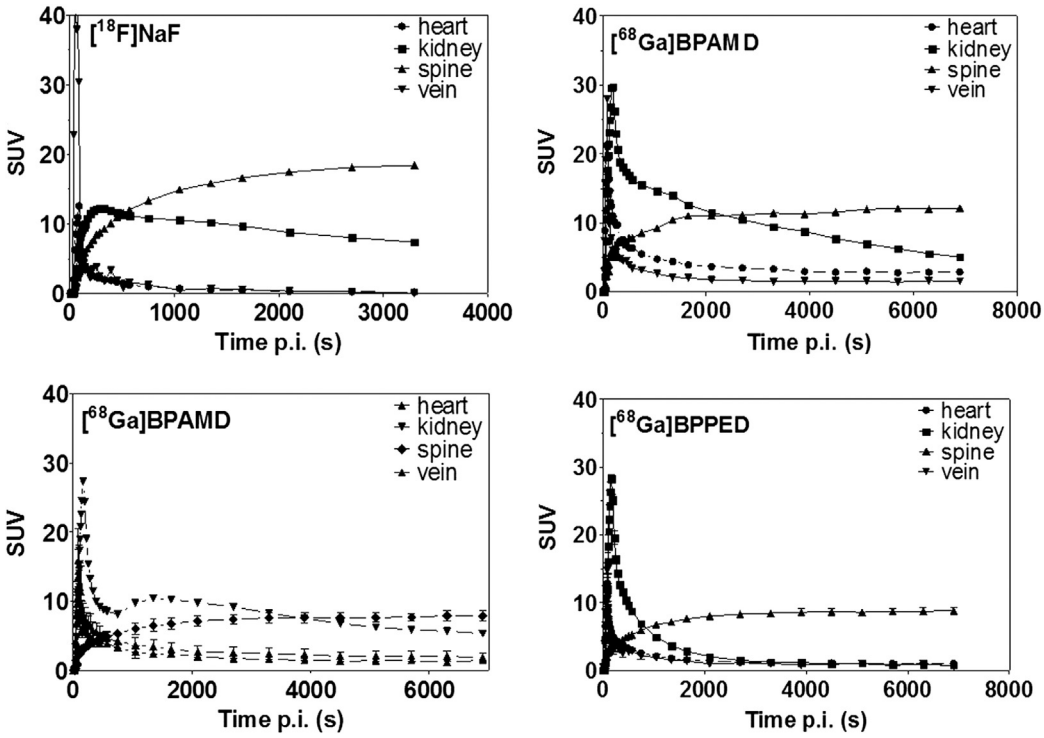

Fig. 5. Time activity curves of ^{68}Ga]BPAMD, [^{68}Ga]BPAPD, [^{68}Ga]BPPED and [^{18} F]F$^-$ in the heart, kidneys, spine and blood stream.

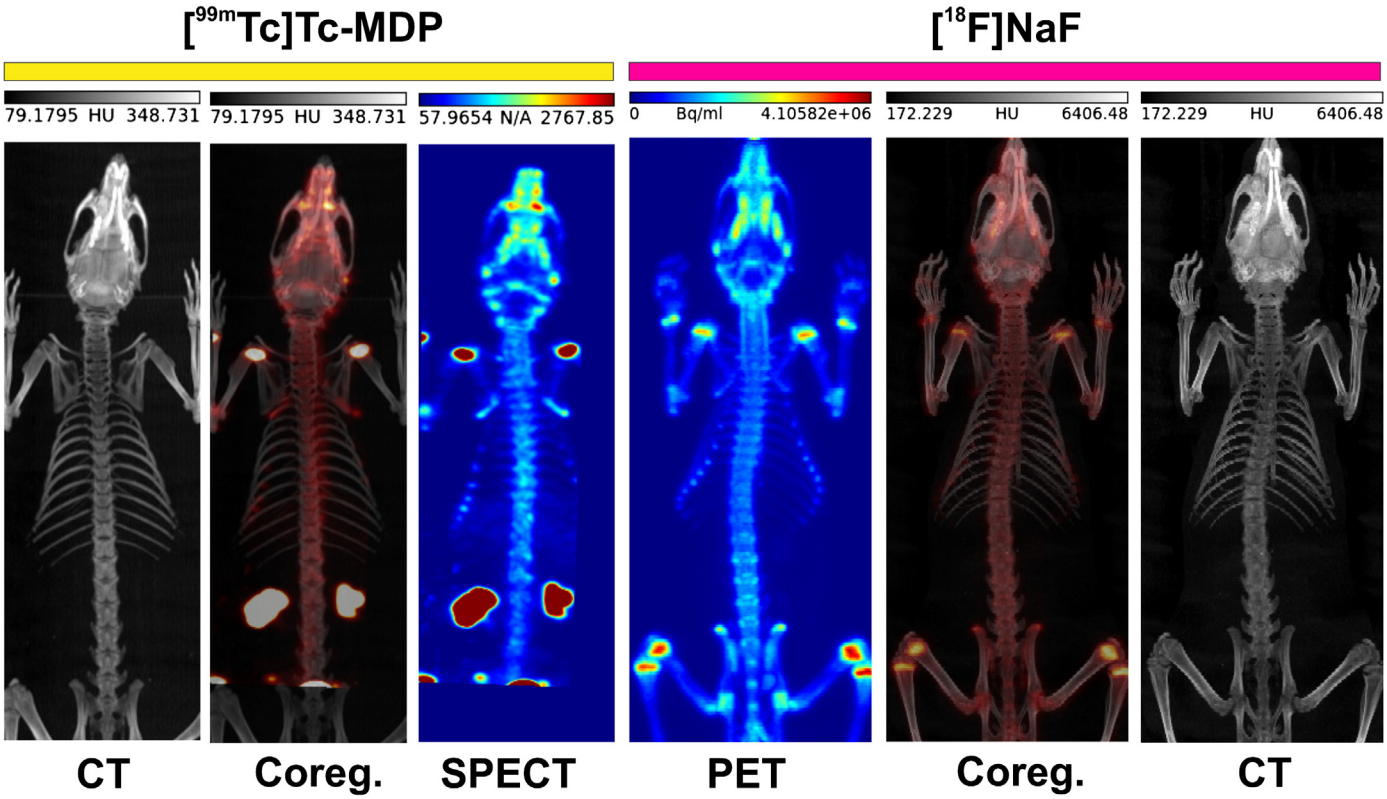

Fig. 6. μPET ([18 F]F⁻, MIP, 60 min p.i.), CT (MIP) and SPECT ([99mTc]MDP, MIP, 120 min p.i.) scans recorded of Wistar rats.

3.4. Metabolite analysis

The metabolism of [68Ga]BPAMD, [68Ga]BPAPD, and [68Ga]BPPED was investigated in arterial blood plasma over one hour. The results are presented in Fig. 7. All three compounds showed similar degrees of decomposition over time. The half-lives of the parent compounds in the arterial blood plasma were 14.4 min (9.3–31.7 min) for [68Ga]BPAMD, 10.2 min (7.4–16.5 min) for [68Ga]BPAPD and 20.8 min for (18.1–24.4 min) [68Ga]BPPED. At 60 min p.i. only about 10% of the plasma activity belonged to the parent compound. This did not have any effect on the blood cell and proteins binding in the arterial blood, where over the observed time about 4–7% were bound to these blood components.

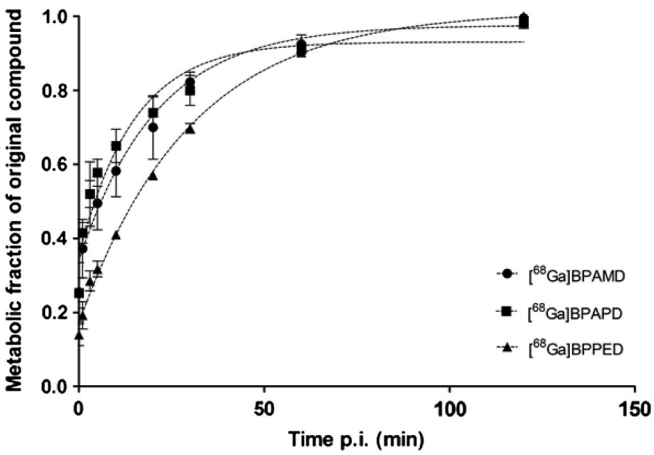

Fig. 7. Metabolic fractions of [68Ga]BPAMD, [68Ga]BPAPD and [68Ga]BPPED analysed in arterial blood plasma at 1, 3, 5, 10, 30, 60 and 120 min p.i.

4. Discussion

The three DOTA based bisphosphonates BPAMD, BPAPD and BPPED have been radiolabeled with 68Ga to give tracers of high radiochemical purity. Each of these tracers showed fast and high binding to the surface of healthy bones. [68Ga]BPPED was the most promising DOTA-based derivative with bone accumulation equal to [18F]F⁻ and [99mTc]MDP, and significantly higher than that of [68Ga]BPAMD and [68Ga]BPAPD. The blood clearance and renal elimination was fast for all compounds investigated. Approximately 90% of the radiolabeled DOTA-bisphosphonates not associated with bone tissue were metabolized within one hour, and eliminated rapidly via the kidneys. These metabolic characteristics produced a very low background from the other organs and tissues. The radiolabeled compounds were not observed in the brain.

The phosphinate conjugated bisphosphonate, [68Ga]BPPED (2.58% ID/g), showed a 20–50% higher accumulation in bone than the two amide compounds [68Ga]BPAMD (2.09% ID/g) and [68Ga]BPAPD (1.68% ID/g). Furthermore, [68Ga]BPPED also showed faster clearance from the blood via the renal system. The main structural difference

Table 3
Bone to blood ratios and the combined activity associated with the urine and skeleton (% ID, mean ± SD of n animals) for [68Ga]BPAMD, [68Ga]BPAPD, [68Ga]BPPED, [18F]F⁻ (at 60 min p.i.) and [99mTc]MDP (at 120 min p.i.).

compound	bone/blood			sum urine + skeleton (% ID)		
	mean	SD	n	mean	SD	n
[68Ga]BPAMD (60 min)	3.42	0.54	8	64.2	12.4	8
[68Ga]BPAPD (60 min)	3.73	0.68	8	73.1	9.3	8
[68Ga]BPPED (60 min)	9.87	1.24	8	80.9	14.7	8
[18F]F⁻ (60 min)	103.0	9.00	4	68.2	4.8	4
[99mTc]MDP (120 min)	52.3	15.6	15	79.4	9.7	6

between BPPED and the other DOTA-bisphosphonates is the presence of a phosphinate group, and it is likely that the different pharmacokinetics observed can be attributed to this feature. It is possible that the presence of the phosphinate provides an additional binding site to hydroxyapatite surfaces, which leads to a higher bone uptake. Furthermore, the acidic phosphinate could be deprotonated and, given its anionic nature, may become involved in ^{68}Ga binding. Regardless of whether the phosphinate oxygen ligates the metal or not, the complex is expected to be more polar (if not have an additional anionic charge) than the other two DOTA-bisphosphonates. This greater polarity may account for the enhanced renal clearance of [^{68}Ga]BPPED.

There was no significant difference in the bone accumulation and blood clearance of labeled BPAMD and BPAPD. Given that these structures only differ in the length of the spacer between the bisphosphonate and DOTA moiety, it is apparent that this has no influence on the pharmacokinetics and bone accumulation of the tracer.

In terms of the ligating moiety, the DOTA-bisphosphonates could be described as hybrids of DOTA and DO3A, both of which have been shown to be effective ligands for the complexation of lanthanide ions [14]. In this respect, these DOTA-bisphosphonates are promising candidates as ^{177}Lu carriers for endoradiotherapy of bone metastases. DOTA-bisphosphonates could potentially be used as theranostic tools for the imaging and treatment of bone metastases [14]. This feature enhances the relevance of DOTA-bisphosphonates and gives them a considerable advantage over both [^{18}F]F$^-$ and [^{99m}Tc]MDP.

In view of a potential application of ^{177}Lu-DOTA-bisphosphonates in therapy, the most important parameters are fast and high binding to the skeleton, combined with a fast blood clearance and non-target tissues (including the kidneys). All of the studied compounds share these parameters, however the best bone uptake and target to background ratio was achieved with [^{68}Ga]BPPED.

^{177}Lu would be ideally suited for the treatment of bone metastases, due to its excellent nuclide parameters: the short β^- range of max. 2 mm does not harm the radiosensitive non-target bone marrow, the non-carrier added production route leads to very high specific activities, and the macrocyclic Lu-DOTA complex is characterized by a high kinetic and thermodynamic stability. Labeling studies and biodistribution experiments with ^{177}Lu DOTA based bisphosphonates in an animal tumor model will be realized soon.

In summary, all of the studied DOTA-bisphosphonates (BPAMD, BPAPD and BPPED) appear to be potentially useful compounds for radiolabeling and application in the diagnosis and therapy of bone metastases. Further investigations should involve similar evaluations in tumor models, to ascertain the affinity of these DOTA-bisphosphonates for bone metastases.

Acknowledgment

We thank Prof. Steinbach for the realization of the animal studies at the Helmholtz-Zentrum Dresden-Rossendorf. We are grateful to Andrea Suhr for developing the metabolite analysis and radiolabeling and to Regina Herrlich for animal handling and biodistribution. We thank Stephan Preusche and Frank Fuechtner for the [^{18}F]fluoride production (all Helmholz-Zentrum Dresden-Rossendorf). Support from Long-Term Research Plan of the Ministry of Education of the Czech Republic (No. MSM0021620857) is acknowledged.

References

[1] Greenlee RT, Hill-Harmon MB, Murray T, Thun M. Cancer Statistics 2001 CA. Cancer J Clin 2001;51:15–36.
[2] Rubens RD. Bone metastases – the clinical problem. Eur J Cancer 1998;34:210–3.
[3] Zettinig G, Dudczak R, Leitha T. Nuklearmedizinische diagnostik der osteomyelitis. J Mineralstoffw 2003;10:20–3.
[4] Harmer CL, Burns JE, Sams A, Spittle M. The value of fluorine-18 for scanning bone tumours. Clin Radiol 1969;20:204–12.
[5] Papapoulos SE. Bisphosphonates: how do they work? Best Pract Res Cl En 2008;22:831–47.
[6] Kubíček V, Rudovský J, Kotek J, Hermann P, Vander Elst L, Muller RN, et al. A bisphosphonate monoamide analogue of DOTA: a potential agent for bone targeting. J Am Chem Soc 2005;127:16477–85.
[7] Fellner M, Baum R, Kubíček V, Hermann P, Lukeš I, Prasad V, et al. PET/CT imaging of osteoblastic bone metastases with ^{68}Ga-bisphosphonates: first human study. Nucl Med Mol Imag 2010;37:834.
[8] Vitha T, Kubíček V, Hermann P, Kolar ZI, Wolterbeek HTh, Peters JA, et al. Complexes of DOTA-bisphosphonate conjugates: probes for determination of adsorption capacity and affinity constants of hydroxyapatite. Langmuir 2008;24:1952–8.
[9] Zhernosekov KP, Filosofov DV, Baum RP, Aschoff P, Bihl H, Razbash AA, et al. Processing of generator-produced ^{68}Ga for medical application. J Nucl Med 2007;48:1741–8.
[10] Asti M, de Pietri G, Fraternali A, Grassi E, Sghedoni R, Fioroni F, et al. Validation of ^{68}Ge/^{68}Ga generator processing by chemical purification for routine clinical application of ^{68}Ga-DOTATOC. Nuc Med Biol 2008;35:721–4.
[11] Fellner M, Baum R, Kubicek V, Hermann P, Prasad V, Roesch F. Macrocyclic ^{68}Ga-bisphosphonates for imaging bone diseases. J Nucl Med 2010;51:563.
[12] Sontag W. Long-term behavior of ^{239}Pu, ^{241}Am and ^{233}U in different bones of one-year-old rats: macrodistribution and macrodosimetry. Human Toxicol 1984;3:469–83.
[13] Chollet C, Bergmann R, Pietzsch J, Beck-Sickinger AG. Design, evaluation and comparison of ghrelin receptor agonists and inverse agonists as suitable radiotracers for PET imaging. Bioconj Chem 2012;23:771–84.
[14] Vitha T, Kubíček V, Hermann P, Elst LV, Muller RN, Kolar ZI, et al. Lanthanide(III) complexes of bis(phosphonate) monoamide analogues of DOTA: Bone-seeking agents for imaging and therapy. J Med Chem 2008;51:677–83.